

Milan MORAVČÍK¹, Martin MORAVČÍK²

TRACK DYNAMIC RESPONSE AT LOW FREQUENCIES – DOMINANT FREQUENCIES

Abstract

The paper is devoted dynamic effects in the track structure - the quasi-static excitation due to moving load, as the important source for the response of track components in the low frequency area ($0 \text{ Hz} < f < 40 \text{ Hz}$). The low-frequency track (the rail) response is associated with periodicity of wheel sets, bogies, and carriages of passage trains. The periodicity of track loading is determined by so called dominant frequencies $f_{(d)}$ at a position x of the track.

Keywords

The quasi-static excitation, moving load, the low-frequency response, the influence factor, dominant frequencies.

1 INTRODUCTION

Dynamic phenomena in a track structure are associated with the operating conditions and are in the direct relation with the vehicle-track dynamic interaction. In concentrating on the track structure the dynamic effects may be divided into two groups:

1. The vibration of railway track structures itself – the vibration of rails, sleepers, the ballast layer, and the embankment.
2. The wave propagation which can cause vibrations in the surrounding of the track and to produce vibrations to adjacent structures and a radiated noise.

The track response is practically accounts in the low-frequency range ($0 \text{ Hz} < f < 40 \text{ Hz}$), the medium- frequency range ($40 \text{ Hz} < f < 400 \text{ Hz}$), and the high- frequency range ($f > 400 \text{ Hz}$). Each frequency range has its characteristic frequencies that influence the dynamic behaviour of the track. All railway track structures (bridges, tunnels) as a track structure as will respond to any form of loading they are exposed to.

Many different theoretical analytical and numerical models are available to simulate the dynamic behaviour of railway tracks to moving trains [4]. The track response due to the moving load is usually focused on the vertical track deflection $w(x, t)$ (the track components - the rail, sleepers, the ballast bed, the embankment and vibration the near track field), or on the vertical track velocity $w'(x, t)$, and the acceleration $w''(x, t)$ of these components. Vibration characteristics vary greatly between a passenger train, a freight train, locomotives, and high speed trains, which yield frequencies of excitation to a broad spectrum. The next main track excitation mechanisms are distinguished as:

The quasi-static excitation due to the moving axle load.

The dynamic excitation due to track irregularities and wheel out of roundness.

¹ Milan Moravčík, Prof., Department of Structural Mechanics, Faculty of Civil Engineering, University of Žilina, Univerzitná 8215/1, 010 26 Žilina, Slovakia, e-mail: mimo@fstav.uniza.sk.

² Martin Moravčík, Doc., Department of Structures and Bridges, Faculty of Civil Engineering, University of Žilina, Univerzitná 8215/1, 010 26 Žilina, Slovakia, e-mail: martin.moravcik@fstav.uniza.sk.

This paper is devoted the first group dynamic effects - the quasi-static excitation as the important source for the response of track components in the low frequency area ($0 \text{ Hz} < f < 40 \text{ Hz}$). The low-frequent behaviour of tracks is affected by the substructure, see Fig. 1, and with the periodicity of wheel sets and requires a specific access of solution, see Fig. 2.

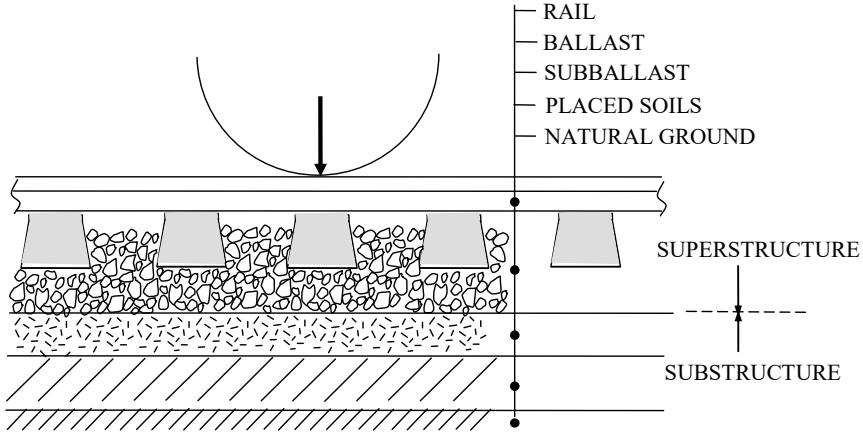


Fig. 1: Ballasted track on soils

The criterions on low-frequency behaviour are either the human perception of discomfort and structural damage of the track due to vibrations. The periodicity of track loading is determined by so called dominant frequencies $f_{(d)}$ at a monitored position x of the track.

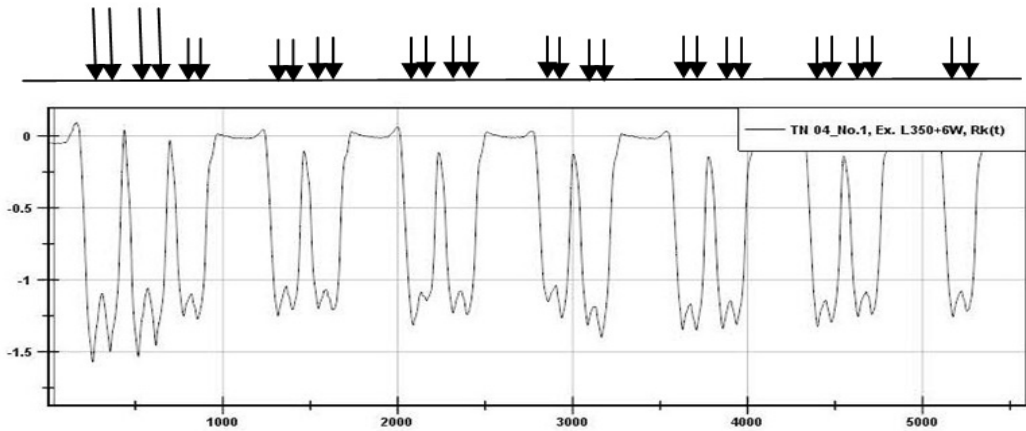


Fig. 2: The measured track deflection $w(x,t)$ due to the passage of the IC train (L350+8W), $c_T=32.2 \text{ m/s}$

To analyse vibration levels for those repeated load, it is important to create a theoretical excitation model taking into account a periodicity of track loading - the travelling a sequence wheel loads $P_{w,j}(c_T, x)$. Such model should be general validity into broader sense of word – for the track on soils, in tunnels, or on bridges, see Fig. 3.

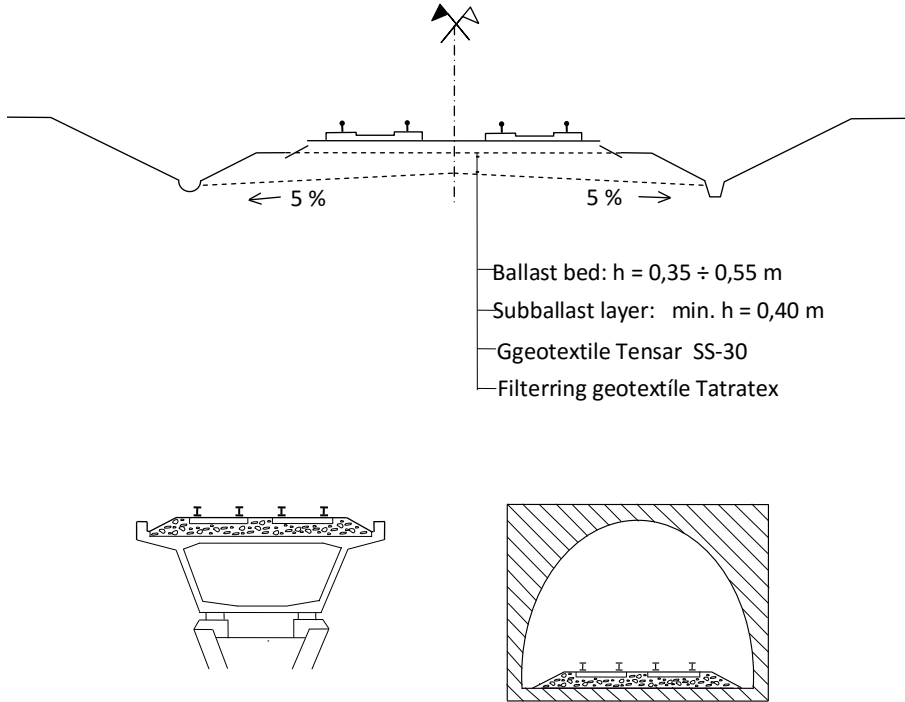


Fig. 3: Ballasted tracks on soils, a bridge, and in a tunnel.

This paper is devoted the first group dynamic effects – the simulation of the track structure vibration due to a moving loading depending on the spacing of the wheel axles, the axle weights and the speed trains. The numerical analyses are applied to provide a right picture on the track vibration and they are compared with experimental results.

2 LINEAR ANALYSIS

For a plain track-foundation model – the Euler-Bernoulli elastic beam laying on the Winkler foundation defined by its stiffness K [kN/m²] per the unit of length (including railpads, ballast, and subgrade), Fig. 4, what is described in detail in numerous literature [4, 6]. This approach is satisfactory for a low-frequency excitation up to 100 Hz. This statement has been confirmed in comparing this theoretical approaches to the FEM model and experimental results.

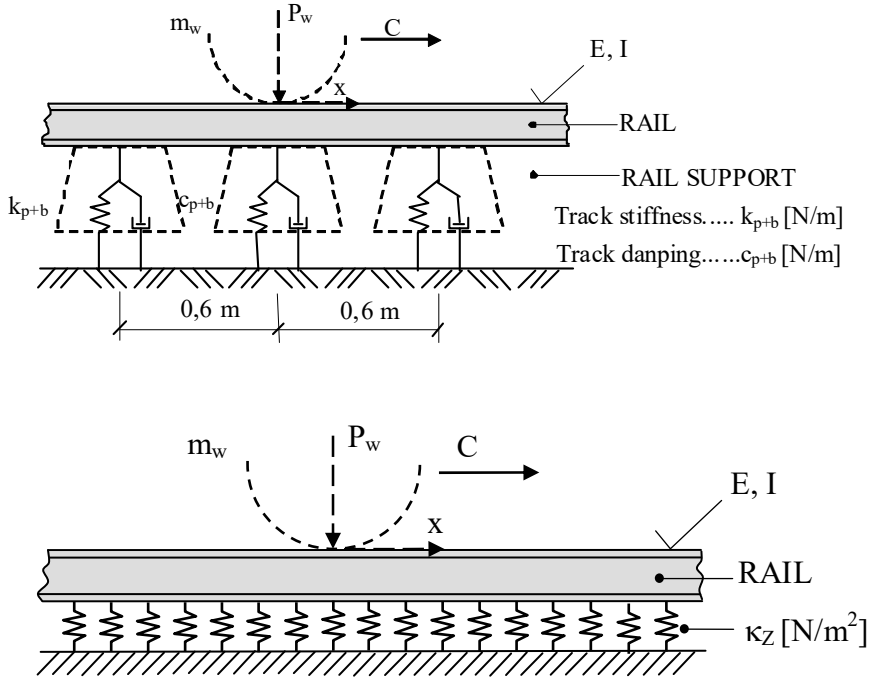


Fig. 4: The single layer track model – Winkler beam on elastic foundation

The vertical track (rail) deflection $w(x, t)$, at the position x and time t , due to a single axle load or a wheel load $P_w(c_T, x)$ that moves with a speed c_T is governed by the partial differential equation:

$$EI_r \frac{\partial^4 w(x, t)}{\partial x^4} + m_l \frac{\partial^2 w(x, t)}{\partial t^2} + \kappa w(x, t) = P_w \cdot \delta(x - c_T) \quad (1)$$

where: EI_r [kNm²] is the flexural rigidity of the rail, for the UIC rail $EI_r = 6.415 \cdot 10^3$ kNm²,
 κ [kN/m²] is the track modulus – subgrade stiffness per unit length,
 m_l [t/m] is the rail mass per unit length.

For a low-frequency excitation neglecting damping (up to 100 Hz) – the quasi-static behaviour of the track is governed by the ordinary differential equation [4]:

$$EI_r \frac{d^4 w(\xi)}{d\xi^4} + \kappa w(\xi) = P_w \cdot \delta(x - c_T \xi) \quad (2)$$

where: $w(\xi)$ is the quasi-static track deflection described in the moving frame of reference $(w(\xi), \xi)$, see Fig. 5, $\xi = x - c_T t$ is the moving coordinate, $\delta(x - c_T \xi)$ is Dirac delta function.

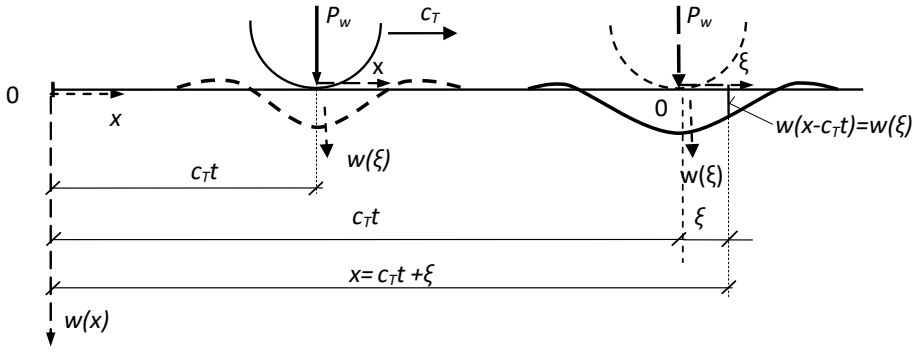


Fig. 5: The quasi-static track deflection $w(x,t)$ due to a single wheel load $P_w(t)$ that moves with the speed c_T

The solution of Eq. (2) can be written as

$$w(\xi = c_T t) = \frac{P_w}{8.EI_r.\beta^3} e^{-\beta|c_T t|} (\cos \beta|c_T t| + \sin \beta|c_T t|) \quad (3)$$

Where: $\beta = \sqrt[4]{\frac{\kappa}{4EI_r}}$ representing a ratio of flexibility between the foundation and the rail,

$A_1 = \frac{P_w}{8EI_r\beta^3} = \frac{P_w}{8.6415,5.\beta^3} = \frac{P_w}{51320.\beta^3}$ is the amplitude of the track deflection (for the UIC rail, $EI_r = 6415$ [kNm²]),
 κ [kN/m²] is the track modulus – the subgrade stiffness per unit length.

The track modulus κ [kN/m²] represents the overall stiffness of the rail foundation (fasteners, railpads ballast, and subgrade) for the Winkler elastic beam model. The relationship between $\kappa \Leftrightarrow k$ is as follows [4]:

$$\kappa = \frac{k^{4/3}}{(64EI_r)^{1/3}} \quad (4)$$

In order to examine the effect of the variable track stiffness conditions the parametric study was created, considering the four subgrade stiffness levels for κ [kN/m²], see Tab. 1.

Tab. 1: Track stiffness levels for the parametric study of the track response.

Track type	Support Stiffnesses	Vertical Track Stiffness κ [kN/m ²]	Characteristics β [m ⁻¹]
A	Low	11 700 ÷ 23 400	0.8203 ÷ 0.9772
B	Medium	23 400 ÷ 46 800	0.9772 ÷ 1.1601
C	Medium	46 800 ÷ 87 700	1.1601 ÷ 1.3565
D	High	87 700 ÷ 117 000	1.3565 ÷ 1.4587

3 LOAD DISTRIBUTION DUE TO A TRAIN PASSAGE USING A SEQUENCE OF CONSTANT AXLE LOAD

To predict the railway track vibration $w_{(T)}(x, t)$ in a place x of the track due to the passage of a complete train (N_c carriages), the moving train load can be estimated as a series of point loads P_w at different locations and different instances of time. Apply such loading series on the track deflection $w_{(T)}(x, t)$ imagines the number of similar events with certain delay times T_j – the passage of car wheels P_w monitored position x , see Fig. 6.

$$w_{(T, N_c)}(x, t) = \sum_{j=1}^{N_c} w_{(P_w)}(t - T_j) \quad (5)$$

Where: $w_{(P_w)}(t - T_j)$ is the vertical track displacement from a j -th single wheel P_w due to the moving at speed c_T .

This situation can be described by means the Dirac delta function $\delta(t - T_j)$. The effect of a single wheel P_w on the track displacement is as follows:

$$w_{(P_w)}(x, t) = w_{(P_w)}(\xi = 0 + c_T t) \delta(t - T_j) = w_{(P_w)}(c_T t) \delta(t - T_j) \quad (6)$$

where: $w_{(P_w)}(\xi = 0 + c_T t) = w_{(P_w)}(c_T t)$ is the vertical track displacement with certain delay time T_j ,

$T_j = \frac{x_j}{c_T}$ with x_j the position of the impulse load, $\delta(t - T_j)$ is the Dirac function for the position of the impulse loading on the track.

Then the travelling of an impulse sequence in time domain $\sum_{j \in N_c} \delta(t - T_j)$ modelling the wheel loads in the track constitute a simple loading model to give the track response $w_{(T)}(x, t)$.

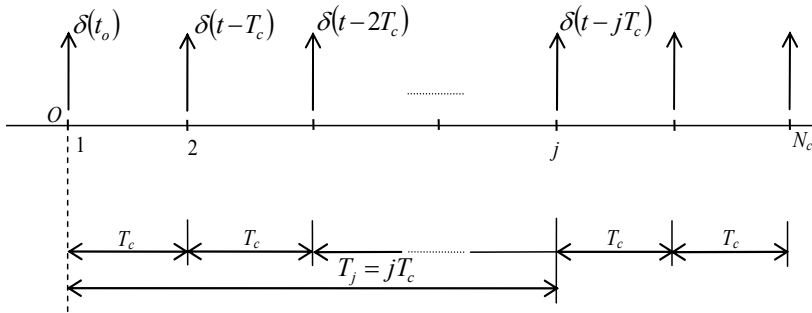


Fig. 6: The impulse loading train $\sum_{j=1}^{N_c} \delta(t - T_j)$

Application of the above consideration due to the train with N_c identical carriages and with N_w wheels in the each carriage is demonstrate in Fig. 7.

3.1 Spectral composition of a sequence of axle loads

If every moving wheel load P_w generates the same vertical displacement response $w_{(P_w)}\delta(t-T_j)$, the total track response $w_{(T)}(x,t)$ due to the train passage with N_c identical carriages and with N_w wheels in the each carriage, see Fig. 7, (accounting the invariance of the geometry in the direction of the track) is given by the superposition:

$$w_{(T,N_c)}(t) = \sum_{j=1}^{N_c} \sum_{k=1}^{N_w} w_{(P_w)}[\delta(t-T_k-jT_c)] \quad (7)$$

Where: N_w is the number of wheels of the identical carriage, N_c is the number of carriages.

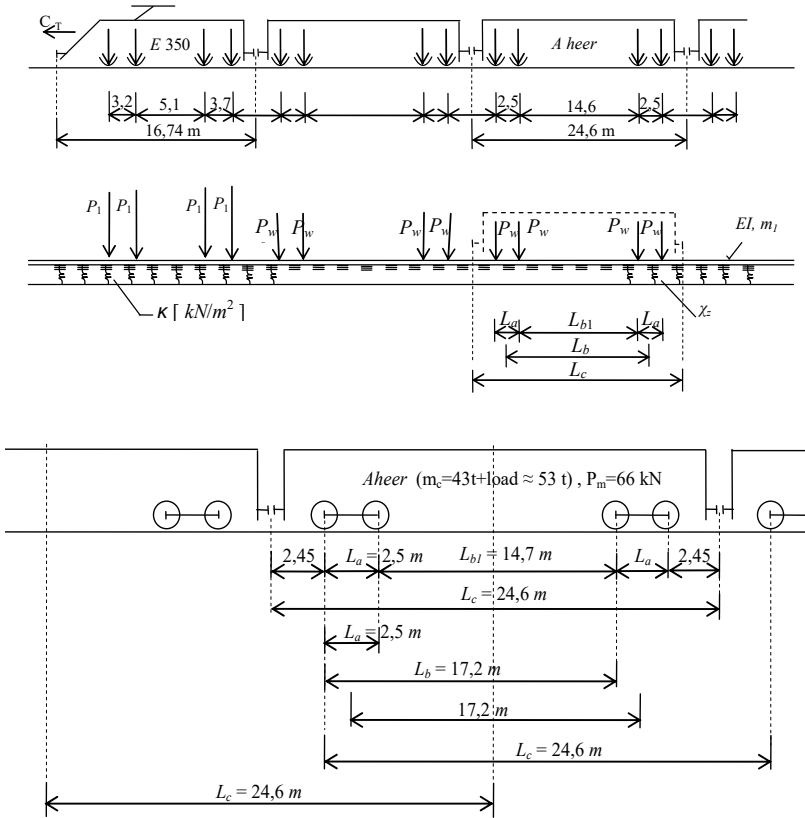


Fig. 7: The IC train with N_c identical IC carriages and with N_w wheels in the each carriage

The Fourier transform (F.T.) of Eq. (7) is:

$$F.T.\{w_{(T)}(x,t)\} \equiv \tilde{w}_{(T)}(if) = \int_{-\infty}^{\infty} \sum_{j=1}^{N_c} \sum_{k=1}^{N_w} w_{(P_w)}(t) [\delta(t-T_k-jT_c)] e^{-i2\pi f t} dt \quad (8)$$

or as the convolution in time:

$$\tilde{w}_{(T)}(if) = F.T.\left\{w_{(P_w)}(t) * \sum_{j=1}^{N_c} \sum_{k=1}^{N_w} \delta(t-T_k-jT_c)\right\} \quad (8a)$$

Eq. (8) can be arranged [2] as:

$$\tilde{w}_{(T, N_c)}(if) = \tilde{w}_{(P_w)}(if) \left((1 + e^{-i2\pi f(\frac{L_a}{c_r})})(1 + e^{-i2\pi f(\frac{L_b}{c_r})}) \left(1 + \sum_{j=1}^{N_c} e^{-i2\pi f \cdot j(\frac{L_c}{c_r})} \right) \right) \quad (9)$$

Eq. (9) can be written in short form

$$\tilde{w}_{(T, N_c)}(if) = \tilde{w}_{(P_w)}(if) \tilde{W}_{(T, N_c)}(if) \quad (10)$$

Where: $\tilde{w}_{(P_w)}(if)$ is again the Fourier Transform of the vertical track displacement $w_{(P_w)}(t - T_k)$ due to the single wheel P_w at the position T_k .

$$\tilde{W}_{(T)}(if) = \left((1 + e^{-i2\pi f(\frac{L_a}{c_r})})(1 + e^{-i2\pi f(\frac{L_b}{c_r})}) \left(1 + \sum_{j=1}^{N_c} e^{-i2\pi f \cdot j(\frac{L_c}{c_r})} \right) \right) \quad (11)$$

In Eq. (11) is applied the time shifting rules [1]:

$$w_{(P_w)}(t - T_k) \Leftrightarrow \tilde{w}_{(P_w)}(if) e^{i2\pi f \cdot T_k} \quad (12)$$

The function $\tilde{w}_{P_w}(if)$ has a character shape asymptotic approaching to zero for $f \rightarrow \infty$, see Fig. 8.

The function $\tilde{W}_{(T)}(if)$ characterizes the loading of the wheel sequence due to the passage of the train with N_c carriages. From the Eq. (11) is derived so called *the influence factor* $R_{(T, N_c)}(f)$ expressing the effect of number N_c carriages on the track response $w_{(T)}(t)$ in the frequency domain:

$$R_{(T, N_c)}(f) = |\tilde{W}_{(T)}(if)| \quad (13)$$

The sum of finite number of phasors in Eq. (11) is the exponential series with a quotient q and after the solution and the modification [6], the sum of phasors (application of Euler relations) gives:

$$\sum_{j=1}^{N_c} e^{-i2\pi f \cdot j(\frac{L_c}{c_r})} = e^{-i2\pi f(\frac{N_c-1}{2})(\frac{L_c}{c_r})} \frac{\sin\left(2\pi f \cdot N_c(\frac{L_c}{2c_r})\right)}{\sin\left(2\pi f(\frac{L_c}{2c_r})\right)} \quad (14)$$

The function $\tilde{W}_{(T)}(if)$, Eq. (11), after exploitation of Eq. (14) and the arrangement gives:

$$\tilde{W}_{(T)}(if) = (1 + e^{-i2\pi f(\frac{L_a}{c_r})})(1 + e^{-i2\pi f(\frac{L_b}{c_r})}) \left(1 + e^{-i2\pi f(\frac{N_c-1}{2})(\frac{L_c}{c_r})} \frac{\sin\left(2\pi f \cdot N_c(\frac{L_c}{2c_r})\right)}{\sin\left(2\pi f(\frac{L_c}{2c_r})\right)} \right) \quad (15)$$

and the corresponding influence factor $R_{(T, N_c)}(f)$ for N_c carriages is defined in the since of Eq. (13) as

$$R_{(T, N_c)}(f) = \left| (1 + e^{-i2\pi f(\frac{L_a}{c_r})})(1 + e^{-i2\pi f(\frac{L_b}{c_r})}) \left(1 + e^{-i2\pi f(\frac{N_c-1}{2})(\frac{L_c}{c_r})} \frac{\sin\left(2\pi f \cdot N_c(\frac{L_c}{2c_r})\right)}{\sin\left(2\pi f(\frac{L_c}{2c_r})\right)} \right) \right| \quad (16)$$

3.2 Single moving wheel effect in frequency domain

The effect of a single moving wheel on the track structure can be represented in the time domain with the Eq. (3). In the frequency domain this effect is described by the Fourier transform:

$$\begin{aligned} F.T.\{w_{(P_w)}(\xi = c_T t)\} &\equiv \tilde{w}_{(P_w)}(if) = \int_{-\infty}^{\infty} w_{(P_w)}(\xi) e^{-i2\pi f \cdot t} dt = \\ &= \int_{-\infty}^{\infty} \frac{P_w \cdot \beta}{2\kappa} e^{-\beta|ct|} (\cos \beta|c_T t| + \sin \beta|c_T t|) \cdot e^{-i2\pi f t} dt \end{aligned} \quad (17)$$

The amplitude spectrum of the quasi-static vertical deflection $w_{(P_w)}(\xi = c_T t)$ of the track due the single wheel P_w is defined as

$$S_{w(P_w)}(f) = |\tilde{w}_{(P_w)}(if)| \quad (18)$$

The amplitude spectrum $S_{w(P_w)}(f)$ has a character shape asymptotic approaching to zero for $f \rightarrow \infty$, see Fig. 8. The amplitude spectrum $S_{w(P_w)}(f)$ for higher train speeds shifts frequency content to higher frequencies. The amplitude spectrum $S_{w(P_w)}(f)$ bounds the total spectrum $S_{w(T)}(f)$ for passage of the train with N_c IC carriages (Chapter 3.1.2).

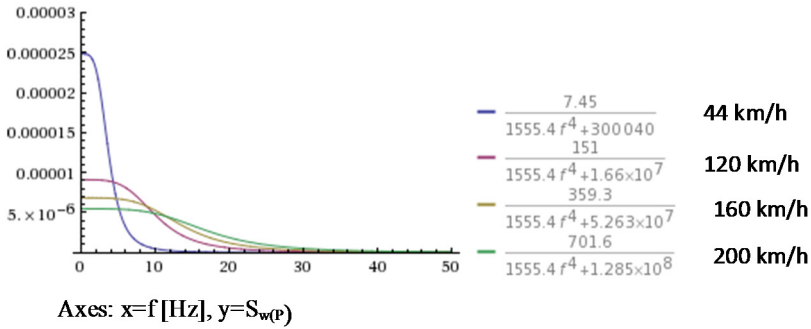


Fig. 8: The amplitude spectrum $S_{w(P_w)}(f)$ of the quasi-static vertical deflection $w_{P_w}(\xi = c_T t)$ of the track under the single wheel $P_w = 66$ kN, the track stiffness $C, \kappa = 87\,700$ kN/m², $\beta = 1.3565$, (Tab.1), and for the speeds $c_T = 12.2 \div 83.3$ m/s

3.3 Passage of the train with N_c carriages

If every moving wheel load P_w generates the same vertical response $w_{(P_w)}\delta(t - T_j)$, the total track response $w_{(T, N_c)}(t)$ due to the train passage with N_c identical carriages and with N_w wheels in the each carriage (Fig. 7), is given by superposition Eq. (7). The Fourier transform of Eq. (7) is given by Eq. (9).

The parametric study for the track response was designed and created to predict the track response with respect the vertical stiffness of the track κ [kN/m²], β [m⁻¹], (Tab. 1), and number of IC carriages $N_c = 5 \div 12$, for $P_w = 66$ kN, for the characteristics of IC carriages ($L_a = 2.5$, $L_b = 17.2$, $L_c = 24.6$). The train speed were considered as: $c_T = 12.2; 33.3; 44.4; 55.5; 72.2, 83.3$ m/s.

3.3.1 Amplitude spectrum, Influence factor, and Dominant frequencies

The influence factor $R_{(T, N_c)}(f)$ and corresponding amplitude spectrum $S_{w(T)}(f)$ of the track (rail) deflection $w(\xi = c_T t, N_c)$, for the passage of the train with N_c carriages, can be expressed by the means Eq. (16,18) as:

$$S_{w(T)}(f) = |\tilde{w}_{P_w}(if) \tilde{W}_{(T)}(if)| = S_{w(P_w)}(f) \cdot R_{(T, N_c)}(f) \quad (19)$$

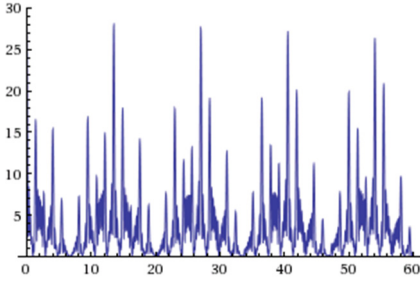
The example of the solved influence factor $R_{(T, N_c)}(f)$ and the amplitude spectrum $S_{w(T)}(f,)$ for the geometrical configuration of IC carriages in Fig. 7 ($L_a=2.5$, $L_b=17.2$, $L_c=24.6$), for $N_c=6$ and 10, and the train speed $c_T=33.3$ m/s, applying of Eq. (16, 19) is displayed in Example 1, Fig. 9a,b. The dominant frequencies $f_{(d)}$ of the vertical displacements $w_{(T, N_c)}(x, t)$ are defined as the relative largest values of the amplitude spectra $S_{w(T)}(f)$.

Example 1 – The example of the major and minor extremes in the amplitude spectra for the IC train, Fig. 9a, b: a/ for $S_{w(T)}(f, N_c = 6)$, b/ for $S_{w(T)}(f, N_c = 10)$. Solution is made for the IC train $c_T=33.3$ m/s, the subgrade stiffness $C_2, \kappa= 87\,700$ kN/m², $\beta=1.3565$ m⁻¹, and the wheel force $P_w = 66$ kN, see Fig. 7.

plot	$\left \frac{(1 + e^{(-0.471239i)f})(1 + e^{(-3.26726i)f})}{(1 + e^{(-11.6239i)f} \csc(2.32478f) \sin(13.9487f))} \right $	$f = 0 \text{ to } 60$ $y = 0 \text{ to } 30$
------	-----------------------------------------------------------------------------------------------------------------------------	--------------------------------------------------

a/ Result $R_{(T, N_c)}(f, N_c = 6) =$

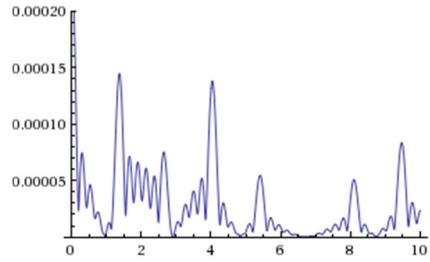
Plot $R_{(T)}(f, N_c = 6)$



Axes: x= f [Hz], y= $R_{(T, N_c)}(f, N_c = 6)$

Dominant frequencies: ^(ex) $f_{(d)} = 0.1; 1.4; 2.6; 4.0; 5.4; 8.1; 9.5$ [Hz]

Plot $S_{w(T)}(f, N_c = 10)$

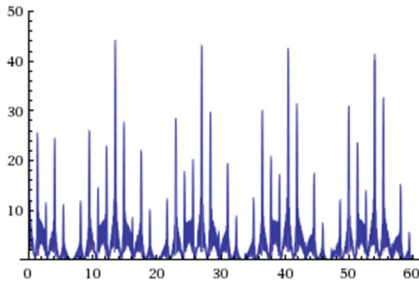


Axes: x= f [Hz], y= $S_{w(T)}(f, N_c = 6)$ [m]

plot	$\left \frac{(1 + e^{(-0.471239i)f})(1 + e^{(-3.26726i)f})}{(1 + e^{(-20.923i)f} \csc(2.32478f) \sin(23.2478f))} \right $	$f = 0 \text{ to } 60$ $y = 0 \text{ to } 50$
------	----------------------------------------------------------------------------------------------------------------------------	--------------------------------------------------

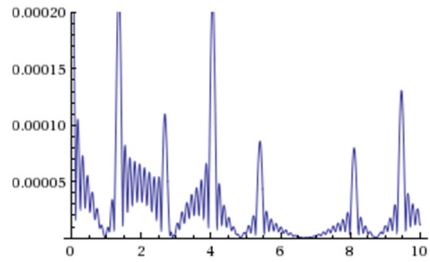
b/ Result $R_{(T, N_c)}(f, N_c = 10) =$

Plot $R_{(T, N_c)}(f, N_c = 10)$



Axes: x= f [Hz], y= $R_{(T, N_c)}(f, N_c = 10)$

Plot $S_{w(T)}(f, N_c = 10)$



Axes: x= f [Hz], y= $S_{w(T)}(f, N_c = 10)$ [m]

Fig. 9: The example of the major and minor extremes in the amplitude spectra for the train a/ for $S_{w(T)}(f, N_c = 6)$, b/ for $S_{w(T)}(f, N_c = 10)$, for the IC train $c_T=33.3$ m/s, the subgrade stiffness $C, \kappa= 87\,700$ kN/m², $\beta=1.3565$ m⁻¹, for $P_w = 66$ kN

Among the main extremes in Fig. 9 is $(N_c - 1)$ points where the function has zero points and between the main extremes is $(N_c - 2)$ side extremes. Increased number of cars amplifies the amplitude of $R_{(T, N_c)}(f)$ and the corresponding amplitude spectrum $S_{w(T)}(f)$ of the track deflection.

The influence factor $R_{(T, N_c)}(f)$ has maxima at a regular spacing

$$\Delta f = \frac{1}{T_{(j)}} = n \frac{c_T}{L_{(j)}} \quad (20)$$

where $T_{(j)} = \{T_a, T_b, T_c\}$ is the time for the passage of a axle T_a , a bogie T_b and a carriage T_c , L_j is a distance between the j th wheel and a adjacent one, n is the positive integer.

The influence factor $R_{(T, N_c)}(f)$ has typical properties resulting from the sequence of wheel loads which are separated by a time delay dependent on the axle distance and the train speed. The frequency content of the first term $S_{w(P_w)}(f) = |\tilde{w}_{(P_w)}(if)|$ in Fig. 8, differs quite from the second term $R_{(T, N_c)}(f)$ in Fig. 9. While the spectrum $S_{w(P_w)}(f)$ depends on the characteristics of the track, the spectrum $R_{(T, N_c)}(f)$ depends the geometrical configuration of carriages ($L_a=2,5$, $L_b=17,2$, $L_c=24,6$), and the train speed c_T .

4 EXPERIMENTAL VERIFICATION

Results of the numerical prediction of the vertical track (rail) deflection are compared with in situ measurements were made on the railway corridor in the line Bratislava – Žilina at the straight section Cífer – Trnava, Fig.10.



Fig. 10: The measured track section in the location Cífer – Trnava

4.1 Track deflection during the passage of IC train

The vertical displacements of the rail ${}^{(r)}w_{(T)}(x,t)$ and the sleeper ${}^{(s)}w_{(T)}(x,t)$ were measured by the relative displacement transducers of the type Bosh, mounted on the fixed reference datum (displacement transducers D_R , D_S) and the B&K piezoelectric accelerometers A_R , A_S , of the type BK 4500 were glued to the rail and the sleeper, see Fig. 11. In Fig. 12a is presented the measured time history of the rail deflection ${}^{(r)}w_{(T)}(x,t)$ at the position x of the track, corresponding to the passage of the IC train (L 350+8 carriages, speed $c = 31.7$ m/s = 114 km/h). In Fig. 12b is the spectral analysis $S_{w(T)}(f, N_c = 6)$ of this time record. This experimental result shows very good accordance between the theoretical prediction of the track deflection $w_{(T)}^{theor}(x,t)$ and the situ measurement results $w_{(T)}^{exp}(x,t)$.

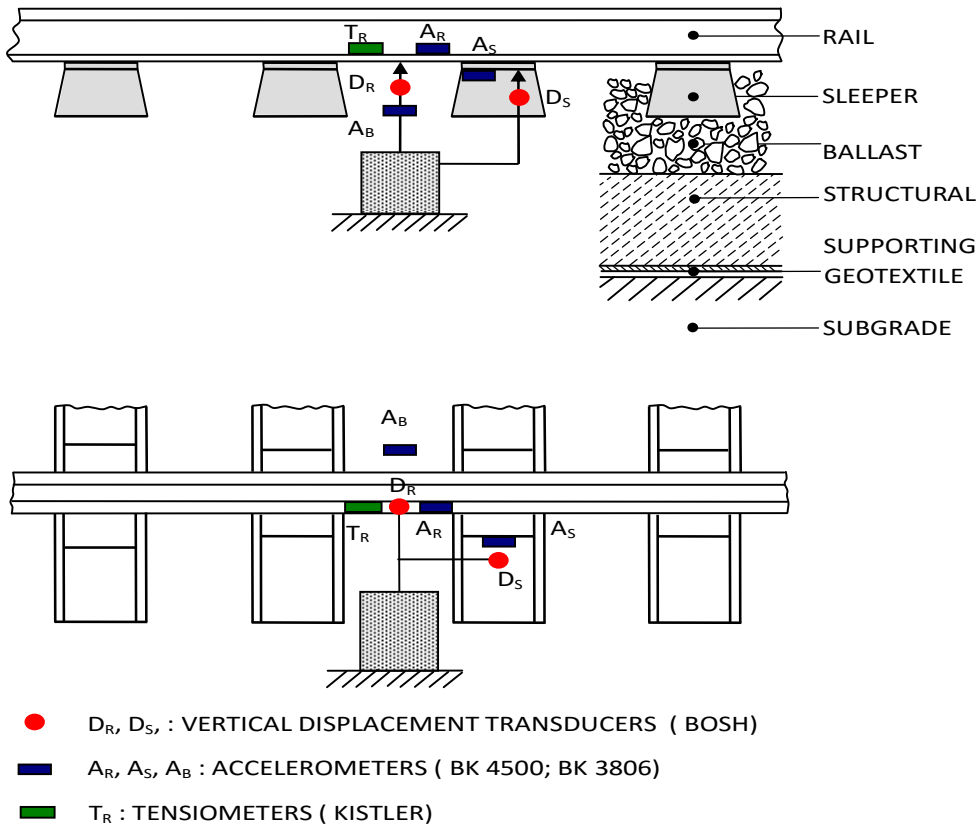


Fig. 11: Scheme of the measurement set-up and positioning transducers in the measured track section Cifer – Trnava

File TN II / No. 2: LABVIEW, $f_s = 1000$ Hz, the non-filtered time records

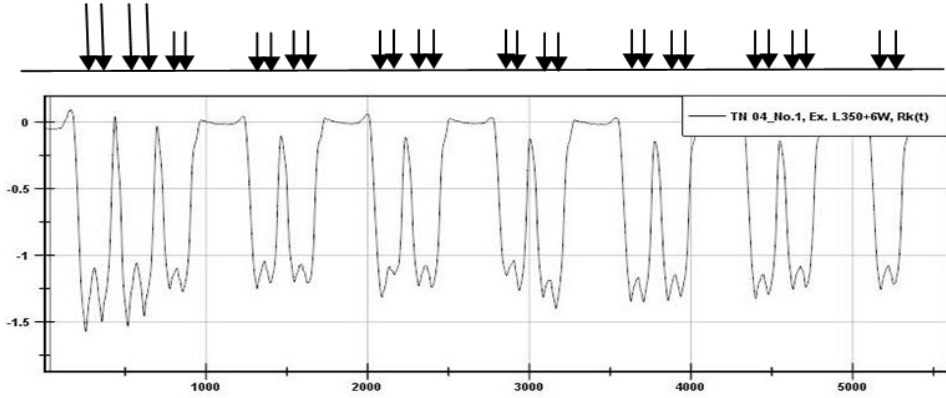
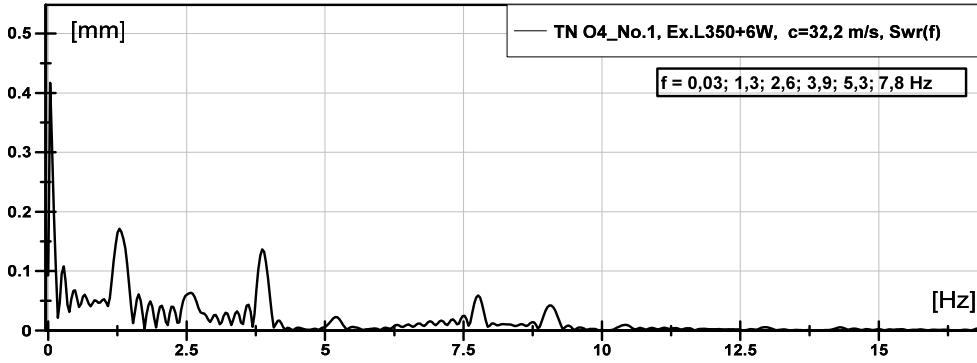


Fig. 12a: Time history $w_{T(N_c=6)}(x, t)$ for IC train (L350+6 carriages), $c_T = 31.7$ m/s

File TN II / No. 2: LABVIEW, $f_s = 1000$ Hz, the non-filtered time records.



Dominant frequencies: $^{(th)}f_d = 0,1 ; 1,30 ; 2,6 ; 4,06; 5,3; 8,1; 9,2; \dots$ Hz.

Fig. 12b: Spectral analysis $S_{w(T)}(f, N_c = 6)$ for IC train (L350+6 carriages)

5 CONCLUSIONS

The quasi-static excitation is the important source for the response of track components in the low frequency area. The track (rail) response is associated with periodicity of wheel sets, bogies, and carriages of passage trains. It is shown that due to the loading sequence of the wheel loads P_w , the frequency content exhibits characteristic dominant frequencies. The dominant frequencies $f_{(d)}$ of the vertical displacements $w_{(T)}(x, t)$ for a passage of the train are defined as the relative largest values of the amplitude spectra $S_{w(T)}(f)$, which are derived from the influence factor $R_{(T, N_c)}(f)$. The dominant frequencies significantly contribute to total vibration of the track components in the low-frequency range ($0 \text{ Hz} < f < 40 \text{ Hz}$).

The numerical analyses are applied to provide a right picture on the track vibration and they are compared with experimental results. The experimental dominant frequencies: $^{(ex)}f_{(d)} = 0.1; 1.4; 2.6; 4.0; 5.4; 8.1; 9.5$ [Hz] and the theoretical dominant frequencies: $^{(th)}f_d = 0.1; 1.30; 2.6; 4.06; 5.3; 8.1; 9.2; \dots$, Hz, for the tested rail deflection $w_{T(N_c=6)}(x, t)$ for IC train (L350+6 carriages), the train speed $c_T = 31.7$ m/s displayed the good accordance. The results confirm the strong attenuation of the amplitudes of vibration due to passage of axle loads to ground vibration near railway tracks.

Results confirm the importance of low frequencies on the mechanical of track components - the rails, sleepers, the ballast bed, and the embankment. In general, the track vibration is influenced by the next dynamic loads, especially due to irregularities on the wheels and rails and the track variations with sleeper-distance frequency.

Analogical approach can be applied to other response quantities of the response in the frequency domain, for example for the vertical track velocity $S'_{w(T)}(f)$, the acceleration of the track $S''_{w(T)}(f)$, or the wheel-rail interaction forces $S_{F_{w-r}(T)}(f)$ applied on the passage of trains with N_c carriages.

ACKNOWLEDGMENT

This work was supported by the project of Slovak Science agency VEGA No.1/0336/15.

REFERENCES

- [1] GLYN James and all.: Edvanced modern engineering mathematics, Pearson Education Limited 1993, 2011, ISBN: 978-0-273-71923-6, 1023 p.
- [2] KATOU M. AND ALL: Numerical simulation of ground vibrations using forces from wheels of a running high-speed train. Journal of Sound and Vibration 318 (2008), pp 830-849.
- [3] KOMRSKA J.: Matematické základy kinematické teorie difrakce: Fourierova transformace mřížky, www.fyzika.fme.vutbr.cz/~komrs/.
- [4] MORAVČÍK MILAN, MORAVČÍK MARTIN: Track Mechanics – Parts 1, 2. – Theoretical analysis and simulation track mechanics problems. (in Slovak), EDIS, Žilina 2002. Part 1, ISBN 80-7100-983-0, 300 p., Part 2, ISBN 80-7100-984-9, 312 p.
- [5] MORAVČÍK MILAN: Dynamic behaviour of railway track – Experimental measurements. Communication 3/2002, ISSN 1335-4205, pp. 45-62.
- [6] TAKEMIYA H., BIAN X.CH.: Shinkansen high-speed train induced ground vibration in view of viaduct-ground interaction. Soil Dynamic and Eartquake Engineering 27 (2007), pp. 506-520.
- [7] WOLFRAM ALPHA: Computational Knowledge Engine, www.wolframalpha.com.

Reviewers:

Prof. Ing. Juraj Králik, PhD., Department of Structural Mechanics, Faculty of Civil Engineering, Slovak University of Technology in Bratislava, Slovakia.

Doc. Ing. Otto Plášek, Ph.D., Institute of Railway Structures and Constructions, Faculty of Civil Engineering, Brno University of Technology, Czech Republic.